

NO-A126 335

TEST OF AN INVERSION ALGORITHM FOR SPECTRALLY RESOLVED
LIMB RADIANCE PROF. (U) ATMOSPHERIC RADIATION
CONSULTANTS INC ACTON MA A S ZACHOR ET AL. 28 SEP 82
AFGL-TR-82-8288 F19628-81-C-8148 F/G 12/1

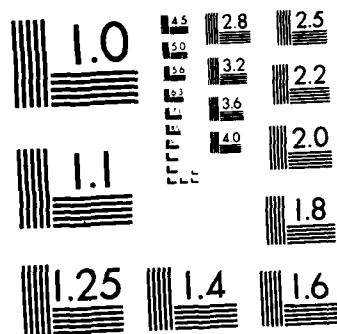
1/1

UNCLASSIFIED

NL

END

FORMED
- 22 -
DTIC

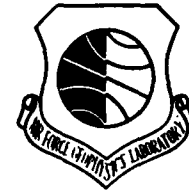


MICROCOPY RESOLUTION TEST CHART
NATIONAL BUREAU OF STANDARDS 1963-A

AD A126335

DTIC FILE COPY

AFCGL-TR-82-0280
PHYSICAL SCIENCES RESEARCH PAPERS, NO. 658



12

Test of an Inversion Algorithm for Spectrally Resolved Limb Radiance Profiles

A.S. ZACHOR
R.D. SHARMA

28 SEPTEMBER 1982

This research was supported by the Defense Nuclear Agency under Subtask 125AAXHX63P, Work Unit 41, Entitled "IR Data Evaluation (FY82)."

OPTICAL PHYSICS DIVISION

PROJECT 2310

AIR FORCE GEOPHYSICS LABORATORY

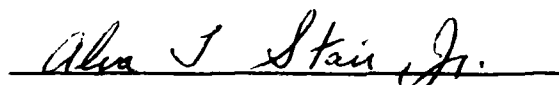
HANSCOM AFB, MASSACHUSETTS 01731

AIR FORCE SYSTEMS COMMAND, USAF



This report has been reviewed by the ESD Public Affairs Office (PA)
and is releasable to the National Technical Information Service (NTIS).

This technical report has been reviewed and
is approved for publication.


DR. ALVA T. STAIR, Jr
Chief Scientist

Qualified requestors may obtain additional copies from the
Defense Technical Information Center. All others should apply
to the National Technical Information Service.

Unclassified

SECURITY CLASSIFICATION OF THIS PAGE (When Data Entered)

| REPORT DOCUMENTATION PAGE | | READ INSTRUCTIONS BEFORE COMPLETING FORM |
|---|----------------------------------|--|
| 1. REPORT NUMBER AFGL-TR-82-0280 | 2. GOVT ACCESSION NO. AD-A126 | 3. RECIPIENT'S CATALOG NUMBER 335 |
| 4. TITLE (and Subtitle) TESTS OF AN INVERSION ALGORITHM FOR SPECTRALLY RESOLVED LIMB RADIANCE PROFILES | | 5. TYPE OF REPORT & PERIOD COVERED Scientific, Interim. |
| 7. AUTHOR(s) A. S. Zachor* R. D. Sharma | | 6. PERFORMING ORG. REPORT NUMBER PSRP No. 658 |
| 9. PERFORMING ORGANIZATION NAME AND ADDRESS Air Force Geophysics Laboratory (OPR) Hanscom AFB Massachusetts 01731 | | 8. CONTRACT OR GRANT NUMBER(s) |
| 11. CONTROLLING OFFICE NAME AND ADDRESS Air Force Geophysics Laboratory (OPR) Hanscom AFB Massachusetts 01731 | | 10. PROGRAM ELEMENT, PROJECT, TASK AREA & WORK UNIT NUMBERS 61102F 2310G415 |
| 14. MONITORING AGENCY NAME & ADDRESS (if different from Controlling Office) | | 12. REPORT DATE 28 September 1982 |
| | | 13. NUMBER OF PAGES 20 |
| | | 15. SECURITY CLASS. (of this report) Unclassified |
| | | 15a. DECLASSIFICATION/DOWNGRADING SCHEDULE |
| 16. DISTRIBUTION STATEMENT (of this Report) Approved for public release; distribution unlimited. | | |
| 17. DISTRIBUTION STATEMENT* (of the abstract entered in Block 20, if different from Report) | | |
| 18. SUPPLEMENTARY NOTES This research was supported by Defense Nuclear Agency under subtask J25AANH53P, Work Unit 14, entitled "IR Data Evaluation of VT20." Atmospheric Radiation Consultants, Inc., 59 High Street, Acton, MA 01720 Research supported under Contract F-19628-81-C-0140 | | |
| 19. KEY WORDS Infrared radiation Spectrophotometry Spectral radiance Spectral radiance profiles | | |
| 20. ABSTRACT Tests of an inversion algorithm are presented that recover vertical atmospheric temperature and temperature by inversion of spectrally resolved limb radiance profiles. The tests, which use synthetic data with known temperature and density profiles, are compared with the results of the inversion algorithm. The results show that the inversion algorithm is capable of recovering the temperature and density profiles of the atmosphere from the limb radiance profiles. | | |

Preface

The authors wish to thank Dr. A.T. Stair, Jr. of the Air Force Geophysics Laboratory for his interest and encouragement in this project.

[illegible]

Contents

| | |
|-----------------------------|----|
| 1. INTRODUCTION AND SUMMARY | 7 |
| 2. RESULTS OF SIMULATION | 10 |
| 3. DISCUSSION | 17 |
| REFERENCES | 18 |

Illustrations

| | |
|---|----|
| 1. Single-peaked Gaussian Model for $\text{NO}^*(\text{H})$ and the (Synthetic) Limb Profile of Band Radiance Determined by $\text{NO}^*(\text{H})$ and the Model Temperature Profile $T(\text{H})$ | 11 |
| 2. Same as Figure 1, Except the Model for $\text{NO}^*(\text{H})$ Is the Sum of Two Displaced Gaussian Functions | 12 |
| 3. Actual and Retrieved Excited Density Profiles $\text{NO}^*(\text{H})$ for the Noise-free Case | 12 |
| 4. Same as Figure 3, Except that the Actual $\text{NO}^*(\text{H})$ Is Represented by the Double-peaked Model | 13 |
| 5. Actual and Retrieved Temperature Profiles | 14 |
| 6. Actual and Retrieved Density Profiles $\text{NO}^*(\text{H})$ for $(S_A/N_A)_{\text{max}} = 500$, Double-peaked Case | 15 |
| 7. Same as Figure 6, Except $(S_A/N_A)_{\text{max}} = 100$ | 15 |
| 8. Retrieved Temperature Profile for $(S_A/N_A)_{\text{max}} = 500$, Double-peaked Case | 16 |
| 9. Same as Figure 6, Except $(S_A/N_A)_{\text{max}} = 100$ | 16 |

Tests of an Inversion Algorithm for Spectrally Resolved Limb Radiance Profiles

1. INTRODUCTION AND SUMMARY

Spectrally resolved infrared radiance profiles of the Earth's limb can be inverted to obtain vertical distributions of temperature and species concentration. The atmosphere below approximately 70 km, where LTE prevails and the undissociated CO_2 distribution is known, can be probed using broadband limb measurements, as demonstrated by House and Ohring,¹ Gille et al.,² Russell et al.,³ and others. The added dimension of spectral resolution offers the potential of obtaining unambiguous information in the non-LTE altitude regime.

The limb spectral radiance profile cannot in general be expressed as a linear function of the vertical temperature and concentration profiles. Consequently, the inversion must generally be performed by some sort of recursive algorithm. Zachor et al.⁴ used a recursive direct nonlinear technique to recover vertical profiles of excited nitric oxide concentration and kinetic temperature above a 100-km altitude from spectral data measured by the rocket-borne SPIRE CVF spectrometer.^{5,6} These inversions used SPIRE data for the NO fundamental band near $5.4 \mu\text{m}$. Comparable results could have been obtained by an approximate linear method because ground state NO is optically thin for tangent paths above ~ 100 km

(Received for publication 27 September 1982)

(Due to the large number of references cited above, they will not be listed here. See References, page 19.)

for the fundamental band. That is, the measured radiance profile and the excited state density profile have a relationship that is approximately linear for this special case. A nonlinear method can be adapted more easily to the general, non-optically-thin case, which is why we chose to use the nonlinear method in our earlier study,⁴ referred hereafter to as ZSNS.

The direct nonlinear method starts with an initial guess for the solution profile, for example, the excited NO vertical density distribution. The corresponding limb radiance profile is computed and then the guess is relaxed according to some measure of the disagreement between the computed and measured limb radiance profiles. The relaxation equation used in the earlier study, Eq. (8) of ZSNS, revises the guess according to ratios of measured and computed radiance values. The process is iterated until the solution profile has converged.

The purpose of this study is to examine further the inversion capabilities of the relaxation method used in ZSNS, and to determine its sensitivity to noise. We were interested particularly in answering the following questions:

- (a) How accurately can the method recover sharply-peaked distributions? In the limb viewing geometry, a layer far below the peak is observed through much denser layers above it.
- (b) How accurately can the temperature profile be recovered when there is noise in the data? The temperature profile recovered in ZSNS had large, noise-like excursions.

These questions were answered by generating synthetic spectral limb radiance profiles and then inverting them, both before and after the addition of normally distributed pseudo-random numbers representing noise. We used the NO fundamental ($\Delta v = 1$) band and assumed that ground state NO is optically thin for the complete range of tangent paths involved in the simulations, which corresponded to tangent heights between 85 and 130 km. Thus, the equations used for the direct computation of radiance, spectral radiance and the relaxed guess are those given in ZSNS. The inversion method modified to handle the non-optically-thin case (and to recover ground state as well as excited state density) would be expected to have a slightly higher sensitivity to noise than will be indicated by the present results.

In the noise-free simulations, the excited NO vertical density profile was represented by a Gaussian function and also by a double-peaked distribution which is the sum of two Gaussians. The simulations with noise used only the double-peaked distribution. The added white spectral noise had two different rms levels, corresponding to maximum S/N's of 500 and 100; these are the signal-to-noise values at the combination of wavelength and tangent height that produces the maximum limb spectral radiance. The spectral resolution was the same as the SPIRE instrument, approximately $0.05 \mu\text{m}$, which resolves the NO band into 13 spectral elements.

The excited NO density profile $\text{NO}^*(\text{H})$ was retrieved by inverting the synthetic limb profile of band radiance (integrated spectral radiance), whereas the temperature inversion used 13 profiles of spectral radiance. As in the ZSNS study, the $\text{NO}^*(\text{H})$ solution and the set of solutions obtained by inverting each spectral radiance profile are combined to obtain the profile $R(\text{H}, \lambda)$, the normalized spectral emission per unit volume as a function of altitude. The normalized spectral emission $R(\text{T}, \lambda)$ was also computed for various temperatures T . A systematic comparison of the retrieved $R(\text{H}, \lambda)$ and computed $R(\text{T}, \lambda)$ s yields the temperature profile $\text{T}(\text{H})$. The initial guess in each of the inversions consisted of a constant (altitude-independent) value.

The results of the simulations are displayed in graphs in the following section. Examination of the results leads to the following conclusions:

- (a) In the noise-free simulations the retrieved $\text{NO}^*(\text{H})$ and $\text{T}(\text{H})$ were nearly identical to the models used to generate the synthetic limb radiance profiles, except at the very lowest altitudes, where the excited density was two orders of magnitude lower than the peak value(s). The errors at the low altitudes are very likely due to the fact that the synthetic radiances were inadvertently rounded to four significant figures. (See Figures 3-5 in Section 2.)
- (b) For $(S/N)_{\text{limb}} = 500$, the excited NO density can be retrieved with high accuracy down to density levels 50 times smaller than the peak. Below this density level, the accuracy degrades rapidly. It appears that the inversion technique we have used is no less accurate at altitudes below the lower NO^* peak than it is above the higher NO^* peak, although the errors tend to be more systematic in the lower altitude range (see Figure 6).
- (c) For $(S/N)_{\text{limb}} = 100$ the errors in retrieved NO^* density profile have the same behavior as for the higher S/N case, except that the retrieved profile is accurate to levels 20 times lower than the peak (see Figure 7).
- (d) The accuracy in retrieved translational temperature degrades rapidly above some upper altitude limit and below some lower limit. However for $(S/N)_{\text{limb}} = 500$ the rms error in $\text{T}(\text{H})$ is less than approximately 10°C over a wide range of altitudes. For $(S/N)_{\text{limb}} = 100$, the rms error is about $10-20^\circ\text{C}$ near the NO^* peaks; the errors become larger than $50-75^\circ\text{C}$ very rapidly as the actual NO^* decreases to less than one-tenth the NO^* peak values (see Figures 8 and 9).

- (e) Examination of the results indicates that the random peak excursions in the retrieved temperature profile at the altitudes of the NO^* peaks are approximately $\pm 5^\circ\text{C}$ for maximum spectral $\text{S/N} = 500$ and approximately $\pm 25^\circ\text{C}$ for $(\text{S}_\lambda/\text{N}_\lambda)_{\text{max}} = 100$. The temperature profile that we retrieved from the SPIRE NO data (see ZSNS) has excursions of $\pm 75^\circ\text{C}$ near the altitude of maximum NO^* , approximately 130 km. This would be consistent with the present simulation results if the spectral signal-to-noise of the SPIRE data for tangent height $H_T = 130$ km was approximately 30 (after the data is averaged over $0.05 \mu\text{m}$ intervals, as done by ZSNS). Examination of the SPIRE data for this tangent height shows that the enhanced $\text{S}_\lambda/\text{N}_\lambda$ is somewhat greater than 30, but probably not more than 60. Hence, the present results support the conclusions by ZSNS that detector noise was the major cause of the noise-like excursions in the temperature profile retrieved from the SPIRE NO data.
- (f) The results emphasize the importance of achieving high signal-to-noise in limb spectral radiance measurements, and also of considering the tradeoffs between spectral resolution and signal-to-noise. This study did not consider the effects of smoothness constraints on the inversion solutions, which might reduce considerably the S/N requirement.

2. RESULTS OF SIMULATION

The single-peaked Gaussian distribution used to represent the excited density profile $\text{NO}^*(H)$ in the simulations is given by

$$\text{NO}^*(H) = 5 \times 10^4 \exp [-(H-115)/5]^2, \quad (1)$$

where NO^* has the units cm^{-3} and the altitude H is in kilometers. The density profile peaks at 115 km and is e^{-1} times the peak value at 110 and 120 km altitude. The double-peaked distribution, given by

$$\text{NO}^*(H) = 5 \times 10^4 \left\{ \exp \left(-[(H-115)/4.3437]^2 \right) + \exp \left(-[(H-100)/4.3437]^2 \right) \right\}, \quad (2)$$

has a relative minimum at 107.5 km, where NO^* is approximately one-tenth the maximum value ($\sim 5 \times 10^4 \text{ cm}^{-3}$) which occurs at 100 km and 115 km.

The translational temperature profile used in the computation of synthetic radiances is the profile given by the Jacchia⁷ model for an exospheric temperature of 1050K (based on the U.S. Standard Atmosphere 1976). The profile is displayed in graphs that compare the model $T(H)$ to the inversion results, which are described below. Figures 1 and 2 show the two different $\text{NO}^*(H)$ models and the corresponding computed limb profiles of band radiance. The 13 computed limb spectral radiance profiles are not shown.

Figure 3 compares the single-peaked "actual" or model NO^* distribution and the corresponding retrieved profile when no noise has been added to the synthetic band radiance profile. However, the synthetic band radiances were rounded to four significant figures before they were inverted. Note that the error is significant only at the lowest altitudes, where $\text{NO}^*(H)$ is less than 0.01 times the peak NO^* . Figure 4 shows that the error has essentially the same behavior for the double-peaked case.

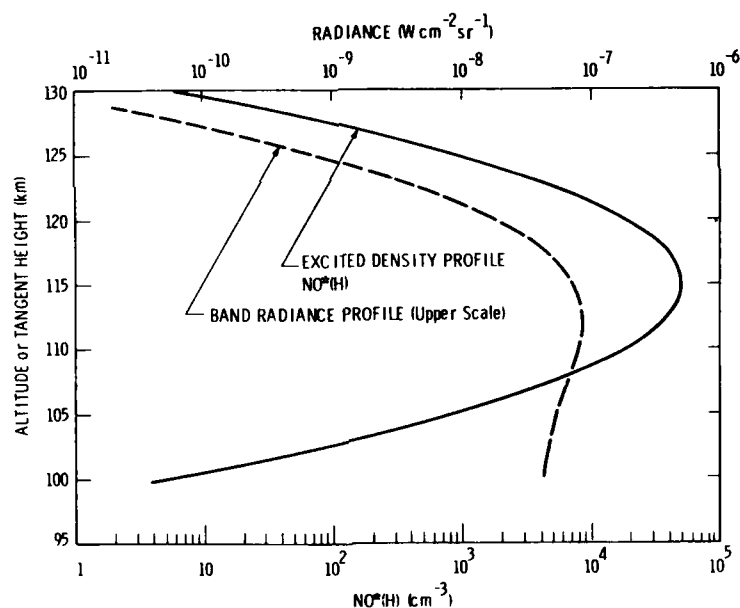


Figure 1. Single-peaked Gaussian Model for $\text{NO}^*(H)$ and the Limb Profile of Band Radiance, Determined by $\text{NO}^*(H)$ and the Model Temperature Profile $T(H)$

7. Jacchia, L. (1977) Thermospheric Temperature, Density and Composition: New Models, Smithsonian Astrophysical Observatory Special Report 375.

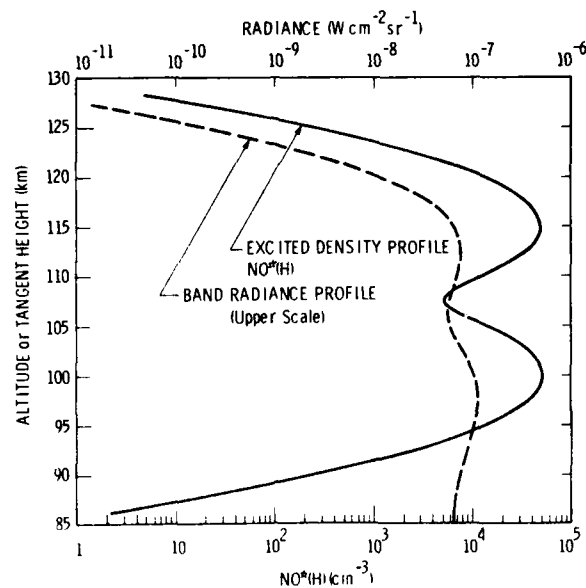


Figure 2. Same as Figure 1, Except the Model for $\text{NO}^*(\text{H})$ is the Sum of Two Displaced Gaussian Functions

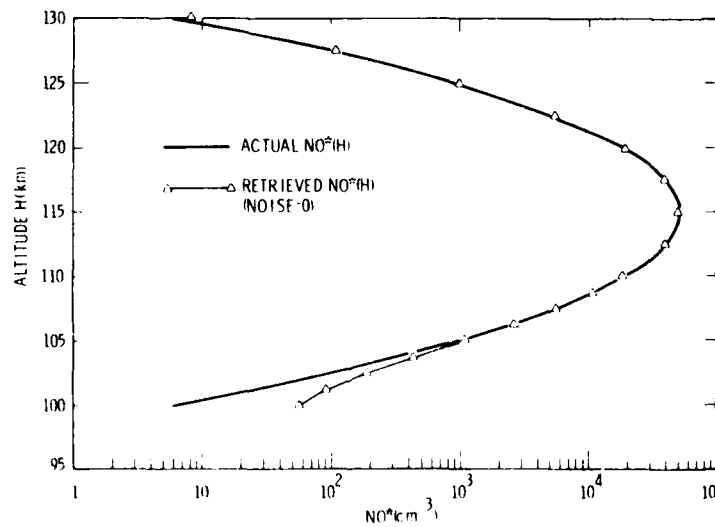


Figure 3. Actual and Retrieved Excited Density Profiles $\text{NO}^*(\text{H})$ for the Noise-free Case. However, the synthetic limb radiance profile was rounded to four significant figures

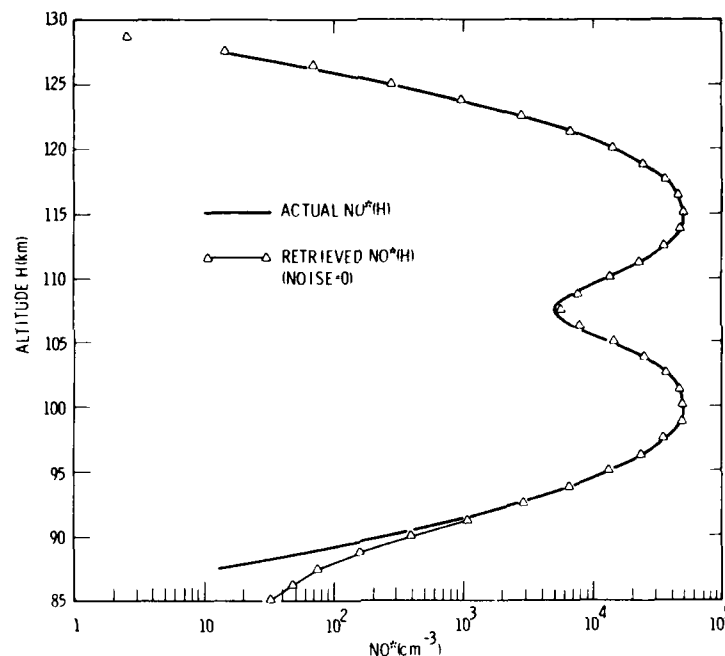


Figure 4. Same as Figure 3 Except that the Actual $\text{NO}^*(H)$ Is Represented by the Double-peaked Model

Figure 5 compares the actual or model $T(H)$ to the temperature profiles retrieved for the single- and double-peaked cases, when only rounding noise is present. The errors in retrieved $T(H)$ are significant at the same altitudes for which the retrieved $\text{NO}^*(H)$ has significant errors, that is, when $\text{NO}^*(H)$ is less than 0.01 times the peak NO^* .

Figure 6 shows the retrieved double-peaked NO^* vertical profile when the maximum spectral S/N is 500. The retrieved profile is in good agreement with the actual profile when $\text{NO}^*(H)$ is greater than ~ 0.01 to 0.02 times the peak NO^* . For a maximum spectral S/N of 100 the actual and retrieved profiles are in good agreement when $\text{NO}^*(H)$ is greater than approximately 0.02 times the peak NO^* ; see Figure 7. However, at 107.5 km where $\text{NO}^*(H)$ has a relative minimum, the relative error is approximately 40 percent.

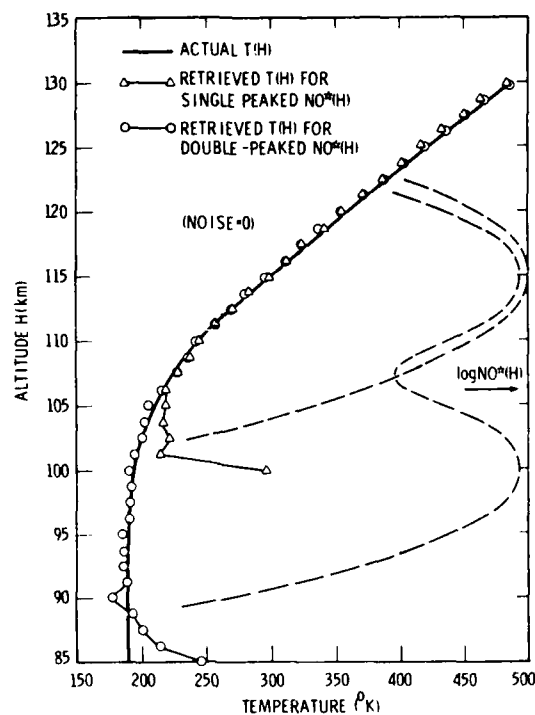


Figure 5. Actual and Retrieved Temperature Profiles. The retrieved profiles are shown for both single-peaked NO^* and Double-peaked NO^* .

Figure 3 shows that accurate temperature profiles can be retrieved over the range of altitudes corresponding to $\text{NO}^*(H) \gtrsim 0.10 \text{ NO}^*_{\text{peak}}$ when $(S_{\lambda}/N_{\lambda})_{\text{max}} = 500$. For the double-peaked model used in the simulations this altitude range is approximately 95-120 km; the error in this altitude regime is less than $\sim 20^\circ\text{C}$.

Figure 4 shows that the retrieved profile has unacceptably large errors when $(S_{\lambda}/N_{\lambda})_{\text{max}} < 100$. The rms error in temperature is less than ~ 10 - 20°C only near the peaks of the NO^* distribution.

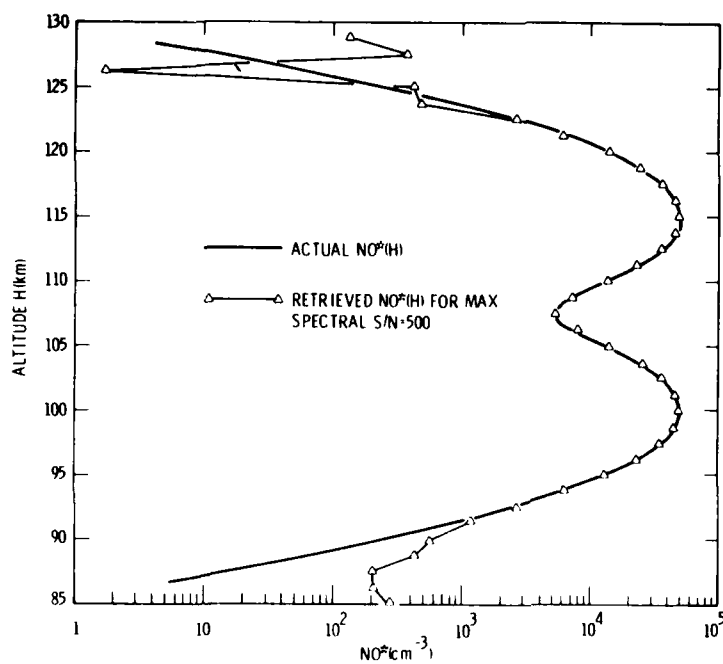


Figure 6. Actual and Retrieved Density
Profiles $\text{NO}^*(H)$ for
 $(S_\lambda/N_\lambda)_{\text{max}} = 500$,
Double-peaked Case

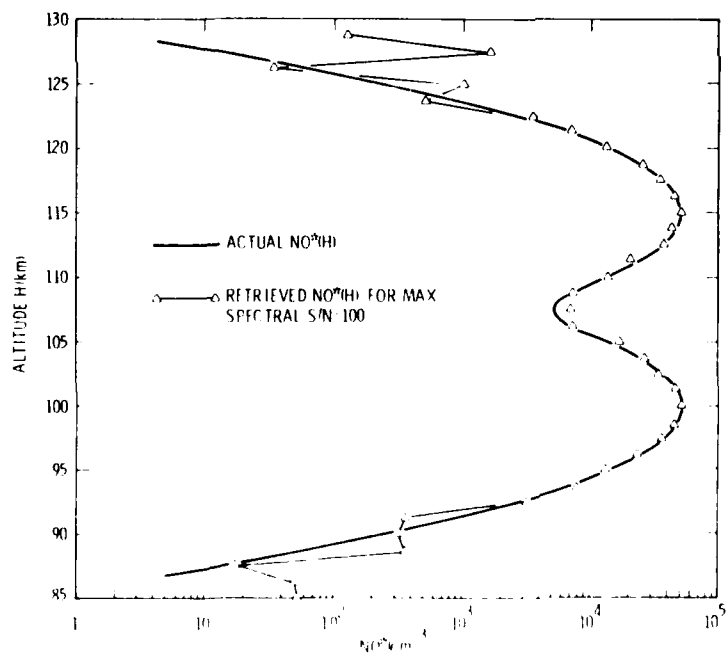


Figure 7. Same as Figure 6, Except
 $(S_\lambda/N_\lambda)_{\text{max}} = 100$

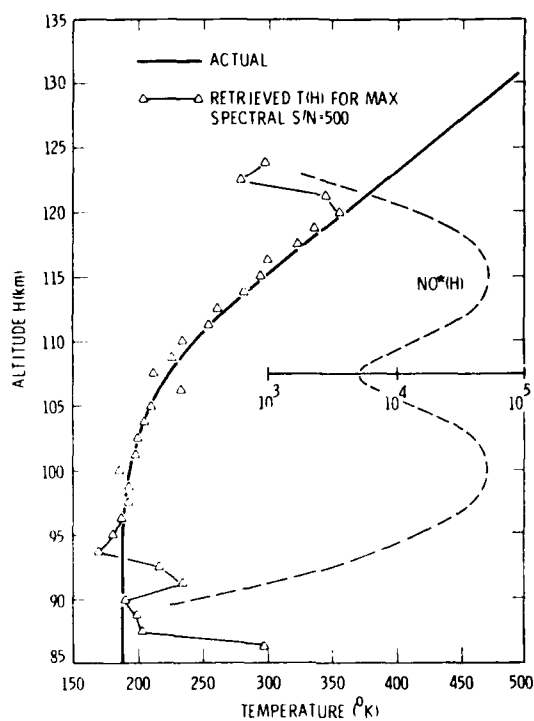


Figure 8. Retrieved Temperature Profile for $(S_{\lambda}/N_{\lambda})_{\max} = 500$, Double-peaked Case

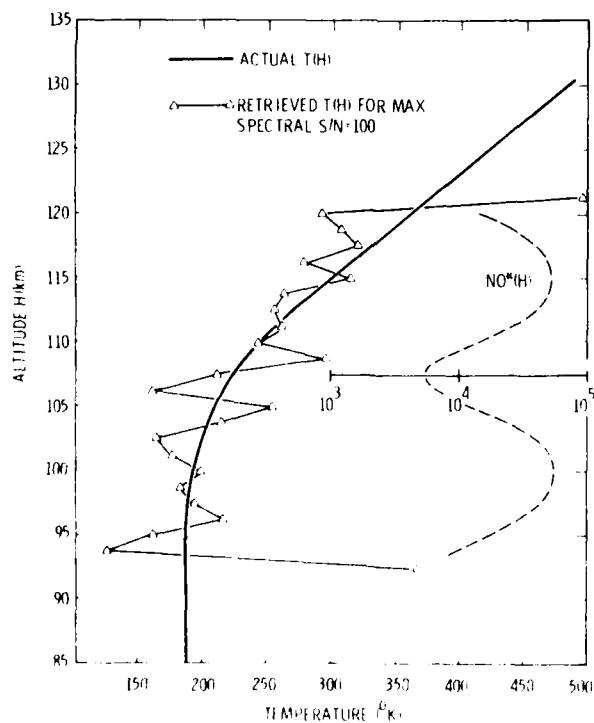


Figure 9. Same as Figure 8, Except $(S_{\lambda}/N_{\lambda})_{\max} = 100$

3. DISCUSSION

It appears that the nonlinear inversion technique investigated in this study is no less accurate below the peak(s) in concentration distribution than it is above the peak(s), although the errors tend to be more systematic at the lower altitudes below a single or double peak.

Based on the results of this study, it is not surprising that the temperature profile retrieved from the SPIRE NO spectral data by ZSNS show noise-like excursions of $\pm 75^\circ\text{C}$. The maximum S_λ/N_λ was between 30 and 60 for the SPIRE data. The present study implies that maximum spectral S/Ns of the order of 500 are required to ensure acceptable temperature solutions.

Translational temperature profiles in the thermosphere have a characteristic smoothness exemplified by the model T(H) used in the simulations. Based on the a priori knowledge (or assumption) of "smoothness", the retrieved temperature profile shown in Figure 9 would be judged "unacceptable". So-called smoothness constraints can be incorporated into the inversion algorithm to significantly reduce the S/N requirement. For the double-peaked NO cases modelled in this study, it is estimated that the S/N requirement can be reduced by a factor as large as two or three.

The study results indicate, nonetheless, the importance of considering the available tradeoffs between spectral resolution and signal-to-noise. High spectral resolution might be required, for example, when two or more species have overlapping spectral bands, or when the available data interpretation algorithm requires resolution of optically-thin portions of a strongly emitting band. When these considerations do not apply one should opt for the minimum spectral resolution that reveals the band contour (translational temperature). The tradeoffs obviously become more complex when the instrument must recover simultaneously the distribution of two or more species.

References

1. House, F. B., and Ohring, G. (1969) Inference of Stratospheric Temperature and Moisture Profiles from Observations of the Infrared H₂O Line, NASA CR-1119, GCA Corp., Bedford, Massachusetts.
2. Gille, J. C., Bailey, P. L., Craig, R. A., and Thomas, J. R. (1975) The limb radiance inversion parameter (LRIP) experiment, in the Nimbus 6 Users Guide, Goddard Space Flight Center, J. E. Stastula, ed., p. 141.
3. Russell, J. M., III, Gille, J. C., Gordley, L. R., and Remsberg, E. E. (1979) The Limb Infrared Monitor of the Stratosphere (LIMS) Experiment: H₂O, NO, and HNO₃ Results, Proceedings of the IYMVP Symposium, Seventeenth General Assembly of the IUGG, 2-15 Dec., 1979, Canberra, Australia.
4. Zachor, A. S., Stastula, R. P., Nault, R. M., and Stupp, A. L., Jr. (1981) Inversion of SPIRE NO Data, MGS-TR-71-0329, AF-103366.
5. Nault, R. M., et al. (1980) SPIRE: Spectral Inversion Experiment, Prog. Space Photochem. Energy Res., 2:141-161.
6. Stupp, A. L., et al. (1981) Final Report on the Components of Aerosol, Ammonia and the Major Atmospheric Gases, AFAT-758, Final Report of the Mission, Science of the Atmosphere, AFAT-758, AF-103366.
7. Zachor, A. S. (1980) Final Report on the Components of Aerosol, Ammonia and the Major Atmospheric Gases, AFAT-758, Final Report of the Mission, Science of the Atmosphere, AFAT-758, AF-103366.

DNA DISTRIBUTION LIST

Air Force Geophysics Lab (AFGL)
Hanscom AFB, MA 01731

Attn: R. Armstrong
W. Blumberg
R. Davis
H. Gardiner
R. Huffman
A. McIntyre
R. Murphy
R. Nadile
R. O'Neil
R. Philbrick
B. Sanford
R. Sharma
A. L. Stair

Air Force Office of Scientific Research
(AFOSR) Bolling AFB,
Washington, DC 20332

Attn: D. Ball
T. Cross

Air Force Space Division
P.O. Box 92960
Worldway Postal Center
Los Angeles, CA 90009

Attn: R. Chadbourne
T. May

Air Force Technical Applications Center
(AFTAC) Patrick AFB, FL 32925

Attn: R. Bigoni

Air Force Weapons Lab (AFWL)
Kirtland AFB, NM 87117

Attn: J. Mayo

Defense Nuclear Agency
Washington, DC 20305

Attn: C. Fitz
P. Lunn
W. McKechney

Aerospace Corp.
P.O. Box 92957
Los Angeles, CA 90009

Attn: J. Crestwell
P. Kisluk
L. Simmons
L. Stocker
L. Sprue
R. Hens
G. Lisle

Electrodynamics Laboratory
Utah State University
Logan, UT 84322

Attn: D. Baker
A. Steed
C. Wyatt

General Research Corp.
Santa Barbara, CA 93111

Attn: J. Ise

General Electric Tempo
816 State Street (PO Drawer QQ)
Santa Barbara, CA 93102

Attn: T. Stephens

Lockheed Missiles and Space Co., Inc.
3251 Hanover Street
Palo Alto, CA 94304

Attn: J. Kumer
R. Sears

Mission Research Corp.
P. O. Drawer 719
Santa Barbara, CA 93102

Attn: D. Archer
D. Sappenfield

Photometrics Inc.
7 Arrow Way
Woburn, MA 01801

Attn: G. Davidson
I. Kovsky

Physical Sciences Inc.
30 Commerce Way
Woburn, MA 01801

Attn: G. Caledonia

R&D Associates
P.O. Box 9695
Marina Del Ray, CA 90291

Attn: F. Gilmore

Space Measurements Lab
Utah State University
Logan, UT 84322

Attn: K. Baker
D. Burt

Space Data Corp.
1333 West 21st Street
Tempe, AZ 85282

Attn: S. Fisher
D. Kushi

DNA DISTRIBUTION LIST (Contd)

Stewart Radiance Lab
Utah State University
Bedford, MA 01730
Attn: R. Hubbi
J. Ulwick

SRI International
333 Ravenswood Ave.
Menlo Park, CA 94025
Attn: W. Chestnut

visi-Tec, Inc.
5 Corp. Place, S. Bedford St.
Burlington, MA 01803
Attn: J. Carpenter
T. Deeges
C. Humphrey
W. Reilly
H. Smith

